Available online at www.sciencedirect.com
SCIENCE DIRECT
Polymer 46 (2005) 11366–11379
polymer
www.elsevier.com/locate/polymer

Rheological evaluation of the influence of polymer concentration and molar mass distribution on the formation and performance of asymmetric gas separation membranes prepared by dry phase inversion

Johannes C. Jansen [a,*], Marialuigia Macchione [a], Cesare Oliviero [b], Raniero Mendichi [c], Giuseppe A. Ranieri [b], Enrico Drioli [a]

[a] *Institute on Membrane Technology, ITM-CNR, Via P. Bucci, Cubo 17/C, 87036 Rende (CS), Italy*
[b] *University of Calabria, Department of Chemistry, Via P. Bucci, Cubo 14/D, 87036 Rende (CS), Italy*
[c] *Istituto per lo Studio delle Macromolecole (ISMAC-CNR), Via E. Bassini 15, 20133 Milan, Italy*

Received 18 April 2005; received in revised form 26 September 2005; accepted 6 October 2005
Available online 27 October 2005

Abstract

Asymmetric gas separation membranes were prepared by the dry-casting technique from PEEKWC, a modified amorphous glassy poly(ether ether ketone). The phase inversion process and membrane performance were correlated to the properties of the polymer and the casting solution (molar mass, polymer concentration, solution rheology and thermodynamics). It was found that a broad molar mass distribution of the polymer in the casting solution is most favourable for the formation of a highly selective membrane with a dense skin and a porous sub-layer. Thus, membranes with an effective skin thickness of less than 1 μm were obtained, exhibiting a maximum O_2/N_2 selectivity of 7.2 and a CO_2/CH_4 selectivity of 39, both significantly higher than in a corresponding thick dense PEEKWC membrane and also comparable to or higher than that of the most commonly used polymers for gas separation membranes. The CO_2 and O_2 permeance were up to 9.5×10^{-3} and 1.8×10^{-3} $m^3/(m^2\,h\,bar)$ (3.5 and 0.67 GPU), respectively.

Keywords: Gas separation membrane; Dry phase inversion; Rheology

1. Introduction

Polymeric membrane formation is a complex process which depends on a great variety of parameters. In the dry–wet phase inversion technique, the most common technique for the preparation of flat membranes, many different factors such as the type and concentration of polymer used, the type of solvent, nonsolvent and additives used in the casting solution and/or coagulation bath, the casting temperature, and for instance the interval between casting and coagulation determine the membrane properties. These factors determine whether the membrane will become dense or porous, symmetric or asymmetric, whether it will have a dense or porous skin and macrovoids or not, and whether it will have a finger-like, sponge-like, cellular or particulate morphology [1–3]. Under different preparation conditions the same polymer may give membranes suitable for different types of separation processes, ranging from microfiltration, ultrafiltration to gas separation, depending on the particular morphology obtained.

In our lab we have studied the membrane forming properties of a glassy poly(ether ether ketone), modified with a cardo group in its backbone (PEEKWC, Scheme 1). The particular structure of PEEKWC makes this polymer, in contrast to the normal PEEK, readily soluble in various common organic solvents at room temperature. It also has good thermal and mechanical properties and is therefore suitable for use as a membrane material [4,5]. This polymer has previously been studied for the preparation of flat [5–7] and hollow fibre membranes [8,9] by wet phase inversion, yielding porous membranes in most cases. Dense PEEKWC is also suitable for gas separation [10,11], and the reported O_2/N_2 selectivity of about 6, and the CO_2/CH_4 selectivity of 33 locate this polymer [5,12–14] above the average in the famous Robeson plot [15].

Most of the polymers commonly used for gas separation membranes are mainly soluble in nonvolatile solvents such as

* Corresponding author. Tel.: +39 984 492031; fax: +39 984 402103.
E-mail address: jc.jansen@itm.cnr.it (J.C. Jansen).

0032-3861/$ - see front matter © 2005 Elsevier Ltd. All rights reserved.
doi:10.1016/j.polymer.2005.10.041

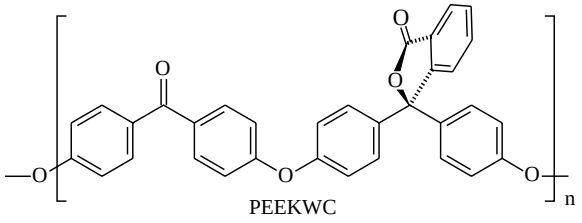

PEEKWC

Scheme 1. Structure of the PEEKWC repeating unit.

N,*N*-dimethylacetamide (DMA), *N*,*N*-dimethylformamide (DMF), dimethylsulfoxide (DMSO) and *N*-methylpyrrolidone (NMP), and membrane preparation methods usually require a wet coagulation step to remove the solvent. In contrast, PEEKWC is also soluble in highly volatile solvents like chloroform, dichloromethane and tetrahydrofuran, enabling film formation by solvent evaporation under mild conditions [7,10,16,17]. Solvent evaporation usually gives relatively thick dense membranes which can be useful for accurate determination of the gas diffusion and solubility coefficients by time lag and/or sorption measurements, but such films are of relatively little practical importance as actual membranes because of their low permeance.

Recently we have presented the preparation of asymmetric PEEKWC membranes with a thin dense skin by the dry phase inversion technique [16,18]. In this method phase inversion is induced by evaporation of the solvent from a ternary mixture of polymer, volatile solvent and nonvolatile nonsolvent and no coagulation bath is required to obtain the asymmetric morphology [3]. It was found that with PEEKWC, using chloroform as the solvent and a series of alcohols as the nonsolvent, the boiling point of the solvent rather than its polarity determines the success of the dry phase inversion technique [16]. In this study it was shown that a less polar and high-boiling nonsolvent gives membranes with a more open porous sublayer and a thinner dense skin than a polar low-boiling nonsolvent. Furthermore, the overall thickness and porosity of the sublayer increases and the skin thickness decreases with increasing nonsolvent concentration in the casting solution, which has its maximum limit at the position of the binodal demixing curve. Besides the casting solution composition, several external parameters determine the membrane formation process. The casting and evaporation temperature acts on the thermodynamics of the phase inversion process through the position of the binodal demixing curve, and on the kinetics of the process through the evaporation rate of the solvent, through the diffusion rate of all species, and through the pore nucleation and growth rate. For the PEEKWC/chloroform/butanol mixture it was found that higher temperatures result in a thicker dense skin [18]. Forced air circulation above the nascent membrane has the same effect, increasing the solvent evaporation rate and reducing the relative pore nucleation and growth rate.

Remarkably the effect of the molar mass distribution (MMD) on the membrane formation and membrane properties has received little attention in the literature, in spite of its strong influence on the properties of the polymer solution. To the best of our knowledge the influence of the MMD has never been studied in the dry-casting process and only few times in the wet-casting or the thermally induced phase separation (TIPS) process, usually in relation to the membrane formation and membrane morphology. In the dry-wet casting of cellulose acetate membranes, a fractionated sample with low molar mass gives denser morphology with courser and less interconnected pores than a sample with high molar mass [19]. Exactly the opposite results were observed by Cheng et al. for polyurethane (PU) membranes prepared by dry-wet casting from a solution in DMF [20]. A high molar mass PU gave a completely dense membrane, both in water and in octanol as the coagulation bath. A low molar mass sample gave a cellular morphology upon coagulation in water and a particulate morphology upon coagulation in octanol. For the PU membranes the limitation of the solvent/nonsolvent exchange at higher molar mass was given as the main reason for the formation of the dense membranes, whereas differences in pore growth kinetics were held responsible for the influence of molar mass on the morphology of the cellulose acetate membranes. In TIPS the morphology was found to change from a cellular structure at low molar mass of the polymer to a sponge-like structure with small, highly interconnected pores at high molar mass [21]. Differences were mainly caused by a strong shift in the cloud point curve and to a faster liquid–liquid phase separation rate; the crystallization temperature remained nearly unaffected by the molar mass. If the differences in molar mass concern the pore forming polymer additive instead of the membrane forming polymer, the effect depends on different factors [22]. If the pore forming polymer has a strong influence on the overall solution viscosity, then for kinetic reasons a high molar mass sample is likely to reduce macrovoid formation. If, on the other hand, the pore forming polymer does not strongly modify the solution viscosity, then its effect as a nonsolvent may dominate and it may promote macrovoid formation. With respect to the final membrane properties, an increase in the molar mass improved the mechanical resistance of a dense chitosan reverse osmosis membrane [23], and it strongly reduced swelling of the dense skin by CO_2 in an asymmetric polyimide gas separation membrane [24].

In the present work we investigated how the MMD and the polymer concentration in the casting solution influenced the dry-casting process and the membrane morphology, and how this could be related to the rheological behaviour of the casting solution. The importance of the polymer solution rheology is evident for continuous membrane preparation processes such as hollow fibre spinning, where flow-induced orientation may be frozen in during the coagulation step [25,26]. In the present work we found that the morphology can be correlated with the MMD and the casting solution rheology even for flat membranes formation through dry-casting, where flow-induced effects are negligible. The aim is to optimize the membrane selectivity and maximize the gas flux, minimizing the skin thickness.

2. Experimental section

2.1. Materials

Analytical grade chloroform, *N*,*N*-dimethylacetamide (DMA) and butanol (BuOH) were supplied by Carlo Erba Reagenti, Italy, and used without purification; PEEKWC was supplied by the Chanchung Institute of Applied Chemistry, Academia Sinica. The chemical structure of PEEKWC is shown in the Scheme 1.

2.2. PEEKWC fractionation

A homogeneous solution of 10 wt% of virgin PEEKWC in DMA was prepared and heated to 50 °C. Under continuous stirring water was added drop-wise to the solution until the mixture became just cloudy. The solution was then slightly heated until it became clear again and cooled down slowly without stirring to allow precipitation of the high molar mass fraction of the polymer. After cooling, the mother liquor was decanted, the precipitated polymer collected, dissolved in about 25 ml of DMA and precipitated in water. The precipitated polymer was filtered and dried under vacuum at 70 °C for 24 h (sample indicated as fraction I).

The mother liquor was heated again to 50 °C and the same procedure was repeated twice more (fractions II and III). After collecting the third fraction the mother liquor remained still very turbid and an additional fraction (IIIa) was obtained by centrifugation of this turbid mother liquor of fraction III. No significant precipitation occurred anymore upon further addition of nonsolvent and the last polymer fraction (IV) was therefore obtained by complete evaporation of the mother liquor of fraction IIIa in a rotary evaporator. Details of the collected fractions are reported in Table 1.

2.3. Size exclusion chromatography

The molar mass distribution (MMD) of PEEKWC was characterized by a multi-detector size exclusion chromatography (SEC) system. The SEC-MALS system consisted of a GPCV 2000 SEC system, using a differential viscometer (DV) and a differential refractometer (DRI) as concentration detector, from Waters (Milford, MA, USA), and an additional multi-angle laser light scattering (MALS) photometer Dawn DSP-F photometer from Wyatt (Santa Barbara, CA, USA). SEC experimental conditions were the following: stabilized tetrahydrofuran (THF) as mobile phase, temperature 35 °C, flow rate 0.8 mL/min and two mixed Styragel HR (5E and 4E) SEC columns from Waters.

The MALS photometer uses a vertically polarized He–Ne laser ($\lambda = 632.8$ nm) and simultaneously measures the intensity of the scattered light at 18 angular locations ranging from 14.2 to 151.9° in THF. The calibration constant was calculated using toluene as standard assuming a Rayleigh factor of 1.406×10^{-5} cm^{-1}. The angular normalization was performed by measuring the scattering intensity of a narrow MMD polystyrene standard ($M_p = 10.3$ kg/mol, $M_w/M_n = 1.03$) in the mobile phase assumed to act as an isotropic scatterer. It is well known that the on-line MALS detector measures, for each polymeric fraction eluted from the columns, the molar mass and when the angular dependence of the scattered light is experimentally measurable also the molecular size, generally known as gyration radius (R_g). In an analogous way the on-line DV viscometer furnishes the intrinsic viscosity [η] of each polymeric fraction and of the whole polymeric sample. The SEC-MALS-DV system was described in detail elsewhere [27,28].

The refractive index increment, $dn/dc = 0.213$ mL/g, for PEEKWC with respect to the THF solvent was measured by a KMX-16 differential refractometer from LDC Milton Roy (Riviera Beach, FL, USA).

2.4. Phase diagrams

The phase diagram of the PEEKWC/$CHCl_3$/butanol mixture was determined by drop-wise addition of alternatingly nonsolvent and solvent under continuous stirring, as described previously [16]. The point of binodal demixing was observed visually for various polymer concentrations as a sudden occurrence of strong turbidity and significant polymer precipitation (upon NS addition) or as a sudden clearing of the mixture and re-dissolution of the polymer (upon solvent addition). This procedure allowed a maximum PEEKWC concentration of about 10 wt%, above which the high viscosity of the solution was prohibitive for efficient stirring and rapid mixing of the components.

2.5. Membrane preparation

Asymmetric membranes were prepared by the dry phase inversion technique according to the method already described

Table 1
Molecular weight averages, gyration radius, R_g, and intrinsic viscosity, [η], of the virgin polymer and fractionated samples, determined in tetrahydrofuran by a multiple detector SEC system

Fraction	M_p (kg/mol)	M_n (kg/mol)	M_w (kg/mol)	M_w/M_n (–)	R_g (nm)	[η] (d*L*/g)
Virgin	53.0	14.0	223.9	16.0	26.3	0.30
Fraction I	89.6	23.1	715.9	31.0	42.7	0.51
Fraction II	218.9	48.4	614.5	12.7	38.1	0.46
Fraction III	40.0	24.2	78.9	3.3	16.7	0.33
Fraction IIIa[a]	40.0	27.7	70.4	2.5	15.7	0.33
Fraction IV	7.3	3.3	10.7	3.2		0.11

[a] Obtained by centrifugation of the mother liquor.

Table 2
Preparation conditions and some macroscopic properties of the prepared membranes

Casting solution		Membrane thickness (μm)		Mass/area (g/m^2)	Porosity, ε (%)	
		SEM	Micrometer[a]		Experimental[b]	Theoretical[c]
PEEKWC concentration[d]	5	26.5	19.2	8	76.7	86.0
(wt%)	7.5	28.5	26.3	11	49.1	80.4
	10	35.8	29.0	16	37.3	75.5
	12.5	32.5	33.0	13	49.4	71.1
	14.6	37.5	39.0	20	38.3	67.8
	7.5[e]	44.8	42.5	18	48.3	76.7
PEEKWC fraction[f]	I[g]	29.2	26.6	10	48.6	70.8
	II	41.7	38.2	15	48.2	71.1
	III	60	65.8	22	53.6	71.1
	Virgin[h]	33	31.0	16	59.4	71.1

[a] Average determined on sample of ca. 15 cm^2.
[b] Based on thickness determined with micrometer.
[c] Calculated from the volume fraction of butanol and PEEKWC in the original casting solution: $\varepsilon_{\text{theoretical}} = V_{\text{BuOH}}/(V_{\text{BuOH}} + V_{\text{PEEKWC}})100\%$.
[d] In chloroform with 20 phr of BuOH.
[e] 16 phr of BuOH.
[f] 10 wt% of PEEKWC in chloroform and 16 phr of BuOH.
[g] 7 wt% of PEEKWC in chloroform and 11 phr of BuOH.
[h] From Ref. [1].

[16]. A thin film of the polymeric solution, including both the solvent and nonsolvent, was cast on a glass plate by means of an opportune knife (Braive Instruments) with a gap of 250 μm. The volatile solvent was then allowed to evaporate at room temperature and atmospheric pressure for at least 16 h. The membrane was released from the glass plate with the aid of a few drops of water and dried under vacuum at 70 °C to remove possible traces of solvent and nonsolvent. Two series of membranes were prepared with varying concentrations of polymer in the casting solution, and with polymers with different molar mass, respectively. Details of the experimental conditions are given in Table 2.

2.5.1. Silicone coating

In order to reduce the effect of pinhole defects (if necessary) the membranes were spray coated with a 5 wt% silicone solution (GE Bayer Silicones, RTV 615) in pentane. Films were dried for 1 h at room temperature and the silicone coating was then cured overnight at 60 °C.

2.6. Rheological characterization and data elaboration

The rheological measurements were conducted using a shear strain controlled rheometer (RFS III, Rheometrics, USA) equipped with a concentric cylinder geometry (inner radius 17 mm, gap 1.06 mm). The temperature was controlled by a heated and refrigerated Circulator, (F32, Julabo, Houston, USA). Samples were fully homogeneous and free from foam and air bubbles during the rheological experiments.

Two different kinds of experiments were carried out: (a) steady flow experiments were performed in a shear rate range of 0.02–1700 s^{-1}. To be sure of steady flow conditions, the flow equilibrium time was measured by transient experiments (step-rate test). It was observed that 10 s was a sufficient time to ensure the steady flow in the system for the entire investigated shear rate range. (b) Dynamic shear experiments were performed in a frequency range between 0.1 and 15.9 Hz. A strain sweep test was carried out before the frequency sweeps in order to guarantee the linear viscoelastic behaviour during the frequency sweep tests. The dynamic strain sweep tests provided information on the linear viscoelastic behaviour of materials through the determination of the complex shear modulus [29].

$$G^*(\omega) = G'(\omega) + iG''(\omega) \tag{1}$$

where $G'(\omega)$ is the in-phase (or storage) component and $G''(\omega)$ is the out-of-phase (or loss) component. The rheological characterisation of the solutions was successfully carried out by using a generalised Maxwell model [30].

According to this theory, the material's viscoelastic behaviour is modelled by a number of Maxwell elements in parallel. A Maxwell element consists of a spring and a dashpot in series, characterized by a spring modulus G^{o} and a relaxation time λ. In a dynamic shear experiment the generalized Maxwell model results in equations for $G'(\omega)$ and $G''(\omega)$ of the form [31]:

$$G'(\omega) = \sum_i \frac{\omega^2 \lambda_i^2 G_i^{\text{o}}}{1 + (\omega\lambda_i)^2} \tag{2}$$

$$G''(\omega) = \sum_i \frac{\omega \lambda_i G_i^{\text{o}}}{1 + (\omega\lambda_i)^2} \tag{3}$$

In this study, the relaxation times (G_i^{o}, λ_i) were obtained by a best fit of the observed viscoelastic moduli to Eqs. (2) and (3). The parameters G^{o} and λ were used as adjustable parameters in an iterative procedure that minimizes the overall standard deviation, $\sigma(G') + \sigma(G'')$. Relaxation times were calculated with an accuracy of $\pm 5\%$.

2.7. Membrane morphology and bulk properties

Surfaces and cross-sections of the asymmetric membranes were observed by scanning electron microscopy (SEM)

(Cambridge Stereoscan 360) at 20 kV. Sample specimens were cryogenically fractured in liquid nitrogen to guarantee a sharp brittle fracture, and were successively sputter coated with a thin gold film before SEM observation.

The thickness of each membrane was directly read from the SEM image of the cross section and was also determined by a multiple-point measurement, using a digital micrometer (Karl Mahr).

The weight per unit area and the overall porosity of each membrane were determined using an analytical balance. The porosity or void fraction, ε, was calculated from the thickness l, the area A and the mass m of the weighed membrane samples:

$$\varepsilon = \frac{V_{\text{void}}}{V_{\text{tot}}} = \frac{V_{\text{tot}} - V_{\text{pol}}}{V_{\text{tot}}} = \frac{lA - (m/\rho)_{\text{pol}}}{lA} \quad (4)$$

in which V_{void} is the void volume, V_{tot} the total specimen volume, V_{pol} the polymer volume and ρ the polymer density, equal to 1.249 g/cm^3 for PEEKWC [14].

2.8. Gas permeability measurements

The ideal gas permeance of the membranes was tested for pure gases at 25 °C and 1 bar of feed pressure by means of an apparatus constructed by GKSS, Germany, according to the procedure described previously [16]. Briefly, the procedure is based on measurement of the pressure increase on the fixed volume permeate side of the membrane cell, with a 34 cm^2 or reduced surface area. Prior to the measurements each membrane was evacuated at 35 °C or higher for about 1 h to guarantee complete removal of dissolved gases or vapours from the membrane and from the sealing rings.

3. Results and discussion

3.1. Polymer fractionation and characterization

The molar mass distribution (MMD) of virgin PEEKWC was studied by size exclusion chromatography, which revealed a very high polydispersity of 16. Careful analysis of the light scattering curve further indicated a slight aggregation of the polymer chains, even in an apparently good solvent such as THF at low concentrations. Similar phenomena form the basis for the relaxation processes observed in rheological evaluation of the casting solutions (see below).

The wide MMD enabled fractionation of the virgin polymer in several fractions with different molar mass averages by a standard procedure of heating, nonsolvent addition and cooling/precipitation [32]. The procedure yielded four different fractions and their MMD is displayed in Fig. 1; numeric values are collected in Table 1. The MMD of the successive fractions shifts to lower values. The first two fractions still have a very wide molar mass distribution because of a shoulder and/or a long tail in the high molar mass range. After the third precipitation step the mother liquor remained very milky and some more polymer was collected by centrifugation of the mother liquor (indicated as fraction IIIa in Table 1).

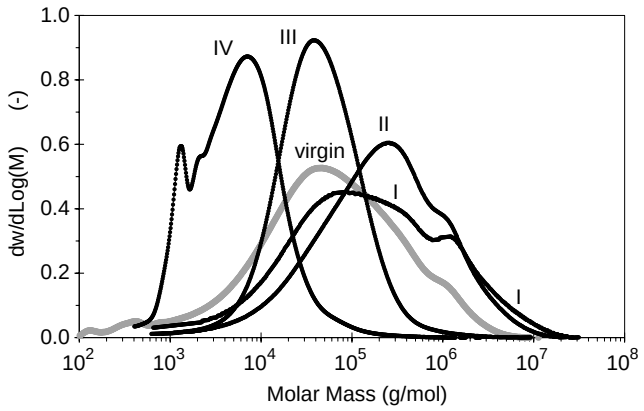

Fig. 1. Molar mass distribution of the polymer fractions and of virgin PEEKWC determined by a multi-detector SEC system.

This fraction has a nearly identical, rather narrow MMD as the spontaneously precipitated fraction (III). The last fraction (IV) was obtained by evaporation of the mother liquor and contains several low molar mass compounds, probably oligomers from the polycondensation reaction. Due to its low molar mass this sample appears to be extremely brittle and is unsuitable for membrane preparation. Fractionation was not particularly efficient in the sense that some of the resulting polymer fractions still had a very wide molar mass distribution. Nevertheless, in absolute terms the MMDs were very dissimilar, inducing significant differences in the behaviour of the fractions during membrane formation.

3.2. Rheological characterization of the casting solution

3.2.1. Influence of the polymer concentration: steady shear experiments

Fig. 2(a) shows the variation of viscosity, η, versus shear rate, $\dot{\gamma}$, for solutions with different polymer concentrations at 18 °C under steady shear flow conditions. It is evident that changes in the polymer concentration induce different rheological behaviour. Samples with a polymer concentration above 10 wt% demonstrate a constant zero-shear viscosity, η_0, at low shear rates; at higher shear rates the viscosity decreases and they behave as typical pseudoplastic systems. The shear thinning behaviour is increasingly pronounced as the polymer concentration increases. This non-Newtonian flow response and the corresponding increase in viscosity with polymer concentration are attributed to the formation and disappearance of entanglements. With increasing shear rate the concentration of entanglements is diminished, primarily because the transit time during which a pair of polymer coils pervade each other's domains as they shear past each other becomes smaller than the time required to form an entanglement. This time required to form an entanglement is proportional to the viscosity η at the existing shear rate [33].

3.2.2. Influence of the polymer concentration: dynamic shear experiments

The viscoelastic properties of the unperturbed system were analysed by oscillatory experiments at 18 °C. Strain-sweep

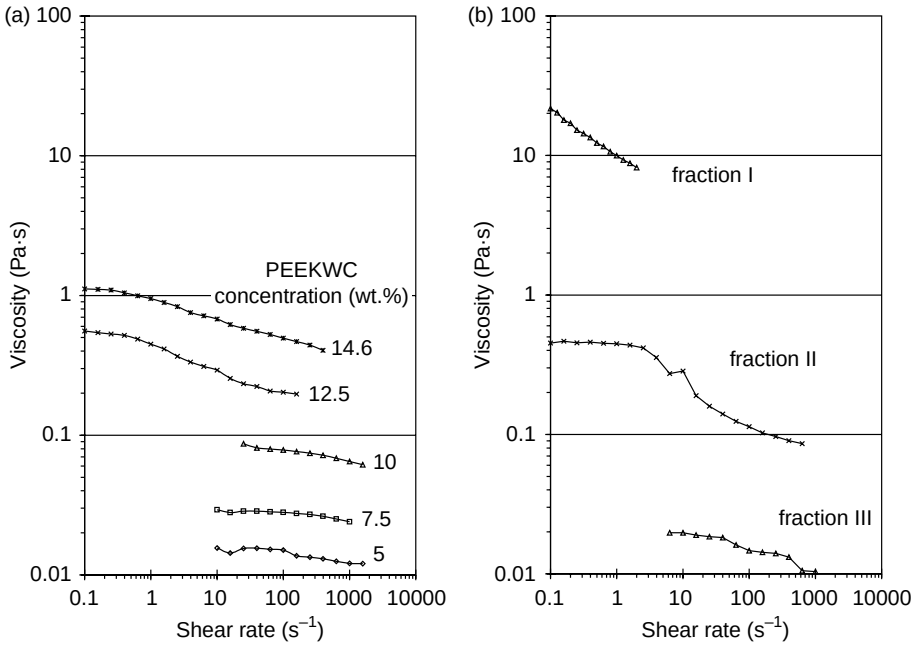

Fig. 2. Steady shear flow curves of casting solutions: (a) with different concentrations of virgin PEEKWC in chloroform with 20 phr of butanol at 18 °C and (b) with polymer fractions of different molar mass at 25 °C (fraction I at 7 wt% with 11 phr of butanol, fraction II and III at 10 wt% with 16 phr of butanol).

tests were performed before each frequency sweep measurement in order to define the linear viscoelastic range and to guarantee the unperturbed conditions of the polymer coils in solution. Moreover, applied pre-shear tests ($10\ s^{-1}$ for 60 s) showed negligible effects on the viscoelastic data of polymer solutions. For all samples both moduli could be measured, although close to the limit of the instrumental resolution, and therefore especially G' became noisier at the lower concentrations. The frequency sweep curves are given in Fig. 3. The reason for the excessive noise of the 7.5% sample is unknown but might possibly be related to overlooked inhomegeneity of the sample.

The viscoelastic properties of the solutions at low polymer concentration can be described well by a single-element Maxwell fluid. With increasing frequency, the storage modulus G' increases faster than the loss modulus G''. If measurements

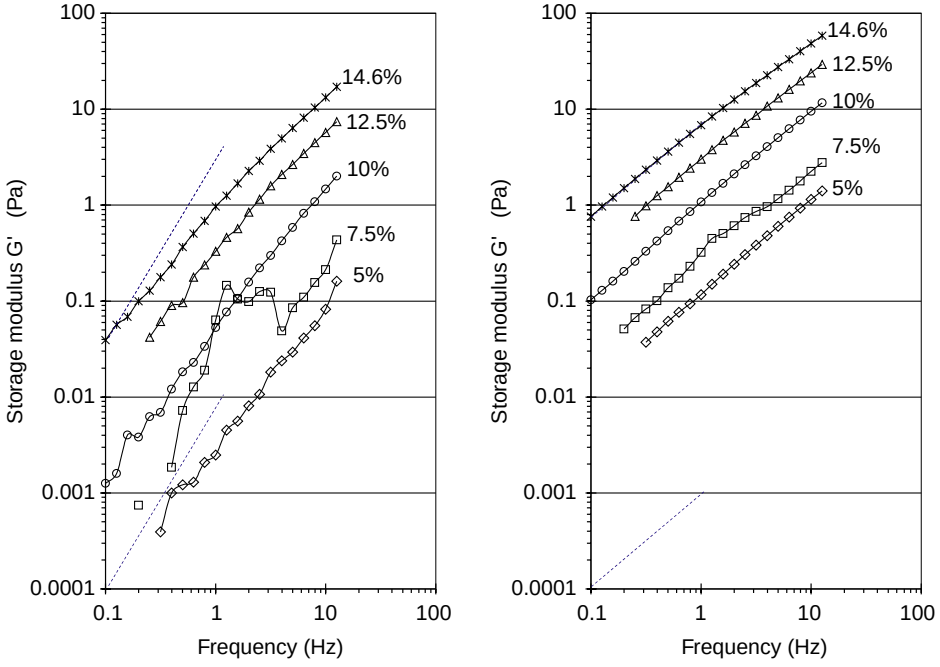

Fig. 3. Frequency sweeps of casting solutions with different polymer concentrations and 20 phr of butanol at 18 °C. Normal slopes of G' and G'' are indicated by a dashed line.

are carried out over a sufficiently wide frequency range the modulus curves intersect at a characteristic frequency, ν_c, depending on the polymer concentration. At the crossover point the modulus functions define a characteristic relaxation time $\lambda = 1/2\pi\nu_c$. The dilute casting solutions have such a short relaxation time that the cross-over point can only be found by fitting the experimental data to a single-element Maxwell model and extrapolation of the fitted data to higher frequencies. It is worth noting that the solutions at relatively low polymer concentration show similar rheological behaviour and that in a log–log plot the slopes of G' and G'' approach the normal slopes of 2 and 1, respectively (Fig. 3). These slope values are typical for polymer solutions where the chains do not touch their neighbours. At higher concentration the slopes change, approaching unity for both G' and G'', and in addition they become frequency dependent, evidencing an interaction between the solute molecules. For the 14.6 wt% casting solution a three Maxwell elements model is required to fit the data.

The viscoelastic data were therefore interpreted in accordance with the theory of Bohlin [34] and Winter [35], reported in the literature as the 'weak-gel model' [36]. This model considers a weak-gel material as a flowing system, characterized by weak physical interactions that cooperatively ensure the stability of the structure. The real structure of this material is made by a cooperative arrangement of flow units to form a stand. The weak-gel model provides a direct link between the microstructure of the material and its rheological properties. The most important parameter introduced is the 'coordination number', z. This is the number of flow units that must interact with each other to give the observed flow response. Coppola et al. [37] showed that the system can be described by the following flow equation:

$$|G^*(\omega)| = \sqrt{G'(\omega)^2 + G''(\omega)^2} = A\omega^{1/z} \tag{5}$$

where A is a constant that can be interpreted as the 'interaction strength' between the rheological units, a sort of amplitude of cooperative interactions. Its dimensions depend on the value of z and are Pa s if z is equal to 1. The values of A and z are obtained by fitting of the experimental data of $|G^*|$ vs ω in a log–log plot, yielding a straight line with slope $1/z$ and intercept A.

Fig. 4(a) shows the concentration dependence at 18 °C of the zero-shear viscosity and of z and A, obtained by fitting the viscoelastic data to Eq. (5). The solutions present a flow coordination number close to unity within the entire concentration range investigated, while the trend of A versus composition shows an evident exponential increase of the interaction strength with increasing polymer concentration. The strong increase in interaction strength is a measure of the number of entanglements [36,37].

Modelling techniques must be used for quantification of the rheological results from oscillatory shear experiments. Several authors have used a generalized Maxwell model to fit viscoelastic data obtained from solutions, using a spectrum of relaxation times [38]. The viscoelastic data of the casting solutions in the present work were thus fitted to Eqs. (2) and (3). Fig. 5 shows the obtained relaxation times as a function of the polymer concentration. At low polymer concentration the dynamics are dominated by a rapid single relaxation (relaxation time ca. 1–10 ms). At these low concentrations no entanglements are present and the observed relaxations must be attributed to the change in the shape of the solute molecules. In the higher concentration range three different relaxations were

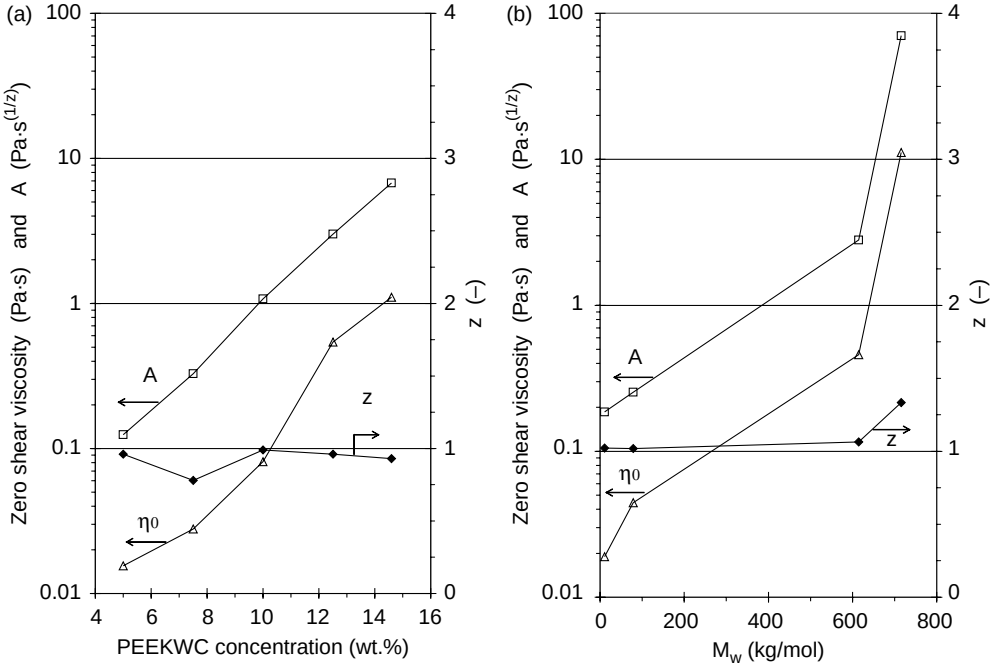

Fig. 4. (a) Concentration dependence and (b) molar mass dependence of the zero shear viscosity, η_0, the coordination number, z and the interaction strength, A, for casting solutions in chloroform. (a) Virgin PEEKWC and 20 phr of butanol at 18 °C; (b) 10 wt% of PEEKWC and 16 phr of butanol at 25 °C.

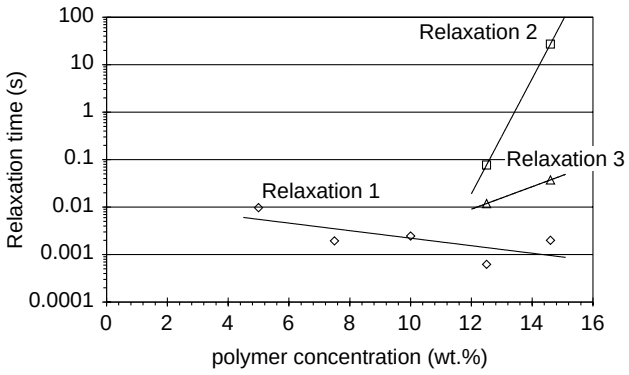

Fig. 5. Characteristic relaxation times for casting solutions with 20 phr of butanol and different polymer concentrations at 18 °C. Relaxation 1, coil deformation; relaxation 2 and 3, reptation and entanglement formation or vice versa.

observed. The shortest time is more or less 1 ms and corresponds to the same coil deformation that occurs at low polymer concentrations. The higher relaxation times indicate the presence of other dissipation mechanisms that must probably be attributed to the formation and destruction of the entanglements and to reptation phenomena, i.e. sliding of chains along one another [29]. At higher polymer concentrations the spatial overlapping of polymer chain segments becomes more likely, thus increasing the number of entanglements and their average lifetime.

3.2.3. Influence of the molar mass

An alternative way to influence the interaction of polymer chains in solution is by variation of the molar mass. While an increase of the polymer concentration brings the dissolved polymer chains closer together, an increase of the molar mass leads to larger coil dimensions of the polymer in solution. Table 1 indeed shows a gradual decrease of the gyration radius from the first, high molar mass sample to the last, low molar mass sample. High molar mass chains are therefore more likely to form entanglements and the effect of increasing molar mass on the rheological properties is thus expected to be similar to that of an increase of the polymer concentration, but without increasing the total solids content of the system.

3.2.4. Steady shear experiments

The flow curves of solutions with different molar mass of the polymer are shown in Fig. 2(b). Newtonian behaviour is observed only for lower molar masses of PEEKWC (fraction III), while at higher molar mass the behaviour tends to become more and more non-Newtonian. For instance, the solution with polymer fraction II has a viscosity plateau up to a critical shear rate of about 2 s^{-1} and a very evident shear thinning behaviour at higher shear rates. With increasing molar mass the Newtonian plateau becomes smaller, it shifts to lower shear rates and the pseudo plastic fluid behaviour becomes more and more evident. The shear thinning behaviour is due to the disruption of the entanglements between different polymer chains with increasing shear rate. Obviously the number and lifetime of the entanglements increases with increasing dimensions of the polymer coils, i.e. with increasing molar mass. It is interesting to note that the effect of molar mass on the viscosity and shear thinning behaviour of the polymer solutions is much stronger than that of the polymer concentration.

3.2.5. Influence of the molar mass: dynamic shear experiments

Also the dynamic rheological experiments as a function of molar mass show similar but even more pronounced behaviour compared to that observed as a function of the polymer concentration. At low molar mass the slope of the G' and G'' curves in a log–log plot tends to the theoretical values for Newtonian liquids of 2 and 1, respectively. For the high molar mass sample I the absolute values of the two moduli increases strongly; they become nearly equal and their slopes tend towards unity (Fig. 6). This indicates that the solution is very close to gelation, which was the reason why a lower polymer concentration had to be used for casting a film of the solution of this sample.

Instead of using a series of Maxwell elements, the relaxation time distribution ($dN/d\lambda$) of the solutions with different molar mass fractions was calculated using the algorithm developed by David Mead and his group at the University of Michigan, incorporated in the Orchestrator software of the rheometer used (Copyright © 2000 Rheometric Scientific Inc). The relaxation spectra of a low and high molar mass sample are shown in Fig. 7. The low molar mass sample has only a very fast relaxation far above the highest shear rate measured, shown as a strong increase in the relaxation intensity at short time. At higher molar mass two additional relaxations appear, with a relaxation time of about 0.8 s and more than 10 s in the case of fraction I.

The nature of the inter-chain interactions was studied by fitting of the viscoelastic data to Eq. (5), using the same procedure described above. Fig. 4(b) shows the molar mass dependence of z, A and the zero shear viscosity. The flow coordination number, z, is close to unity within the entire molar mass range, while the coordination strength, A, increases exponentially with increasing molar mass. Only for the sample with the highest molar mass the coordination number increases above unity and the coordination strength increases more rapidly than the overall trend. This is probably due to the presence of a small amount of polymer with extremely high molar mass (>10 million g/mol), which favours the formation of particularly strong and possibly multiple entanglements. It is evident that the viscosity follows exactly the trend of the coordination strength, as a consequence of the constant value of z.

Summarizing: the overall effect of a molar mass increase of the polymer on the rheological properties of the solution is similar but much stronger than that of an increase in the polymer concentration. The fundamental difference, interesting in view of the membrane formation, is that changes in the molar mass of the polymer allow the variation of the rheological properties of the solution at parity of the solids content. The latter may be important for the overall porosity (void fraction) of the membranes and for their skin thickness.

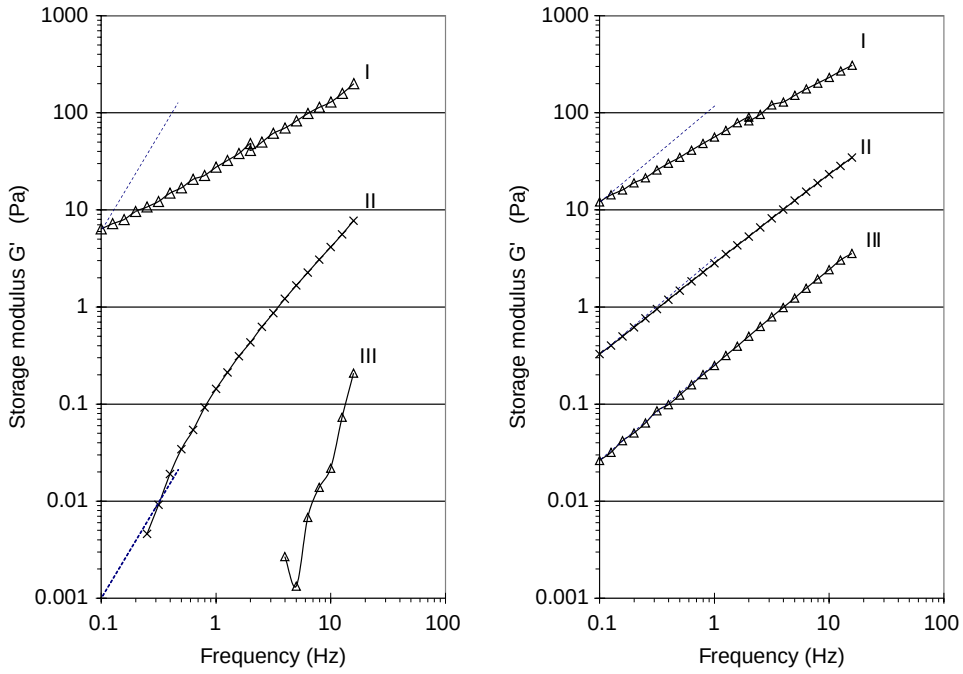

Fig. 6. Storage and loss modulus in frequency sweeps of casting solutions at 25 °C containing three PEEKWC fractions of decreasing molar mass. Polymer concentration 10 wt%, BuOH concentration 16 phr. Normal slopes of G' and G'' are indicated by a dashed line.

3.3. Membrane formation and morphology

A typical velocity of the casting knife is about 1–5 cm/s, corresponding to a shear rate of 40–200 s^{-1} for a gap of 250 μm between casting knife and glass support. This is well within the range where shear thinning occurs for the highest polymer concentrations and the highest molar masses (Fig. 2(a) and (b)) and it is obvious that some orientation of the coils occurs during the casting process. However, typical times observed for the phase inversion to set in are in the range of 0.5–1 min, which is far higher than the longest relaxation times observed (Figs. 5 and 7). Although the relaxation times increase as a result of the increasing polymer concentration during solvent evaporation, it is still likely that most of the shear induced orientation of the casting solution relaxes completely before phase inversion. Therefore, knowledge of the rheological behaviour of the casting solution is most relevant for understanding the phase inversion process itself.

3.3.1. Influence of polymer concentration on the morphology

The influence of the polymer concentration on the membrane morphology was studied by SEM analysis of

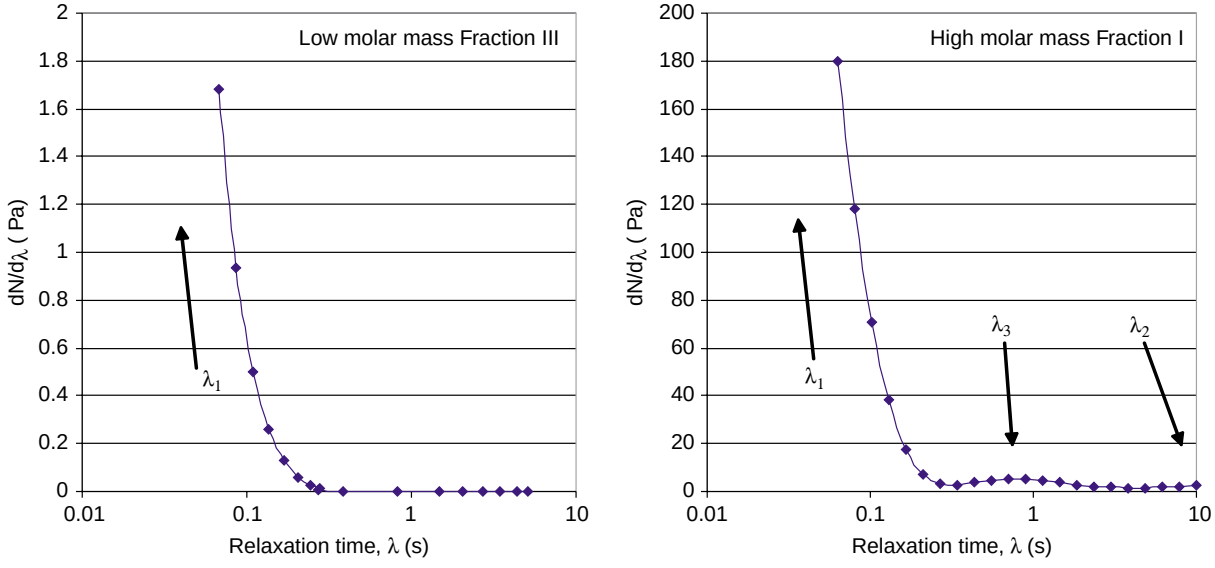

Fig. 7. Relaxation time spectra of the casting solutions at 25 °C with the low molar mass polymer Fraction III (10 wt% PEEKWC, 16 phr butanol) and the high molar mass polymer fraction I (7 wt% PEEKWC, 11 phr butanol).

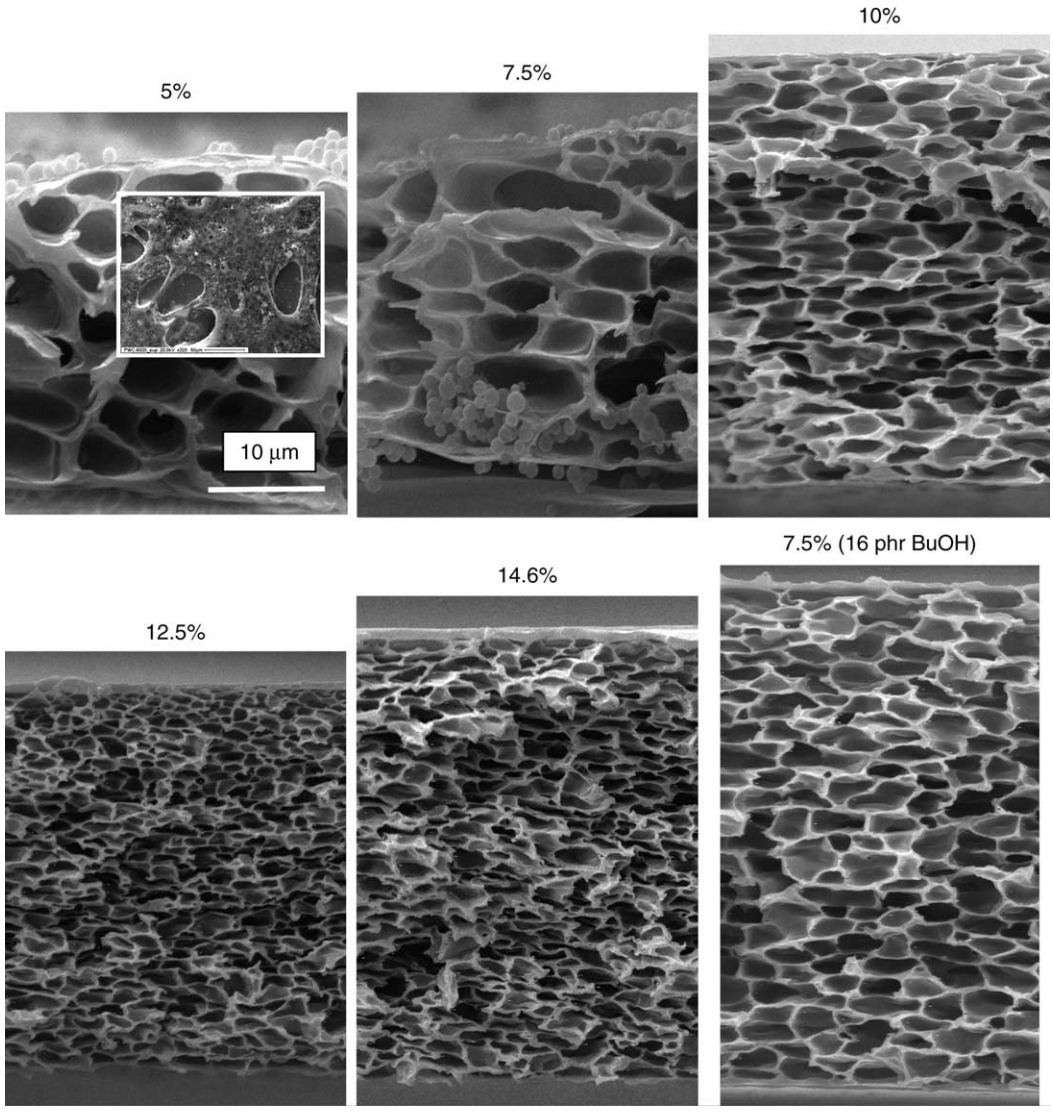

Fig. 8. SEM images of the cross section of membranes prepared with different PEEKWC concentrations and 20 phr of butanol in the casting solution. Insert in the 5% sample: panoramic view of the skin surface at 1/15th of the magnification of the cross section images.

the membrane cross sections (Fig. 8). All membranes present a nearly symmetric cellular morphology with a dense skin. The cell dimensions decrease with increasing polymer concentration. This indicates that nucleation of the polymer lean phase is the main phase inversion mechanism. At 5 and 7.5% of polymer one can also observe the presence of micrometer-sized spheres. These are formed in the second stage of the membrane formation process, when the solvent from the polymer lean phase evaporates. The latter, still containing low concentrations of dissolved polymer, undergoes a second nucleation step, now of the polymer rich phase. In this step small polymer droplets are formed which remain as small spheres after complete evaporation of the solvent and nonsolvent from the membrane. This is a slightly different mechanism than that in the dry-wet phase inversion method, where a similar phenomenon is sometimes observed. In that case the formation of this so-called 'filter dust' is attributed to the delayed precipitation of low molar mass polymer fractions from the polymer lean phase when the latter is expelled from the pores into the coagulation bath [39]. Below 10 wt% of polymer the voids are very large and the skin presents many macroscopic defects, in particular at 5 wt%, as shown by the insert in the image of the cross section. This is due to the low viscosity and the poor film-forming properties at low polymer concentrations, as described above. After nucleation of the polymer lean phase, the low viscosity allows a rapid pore growth. The polymer concentration remains relatively low and little or no gelation of the polymer rich phase occurs even upon further evaporation of the solvent. Finally, the rapidly growing internal pores may therefore cause the skin to break into macroscopic defects. With decreasing polymer concentration the overall porosity or total void fraction increases (Table 2).

This behaviour can be illustrated on the basis of the phase diagram of the PEEKWC/chloroform/methanol ternary mixture (Fig. 9(a)). In the present work the binodal demixing curve of the virgin polymer was determined by a similar titration method as that reported by Schneider et al. [40] but with visual rather than electronic observation of the turbidity changes, as

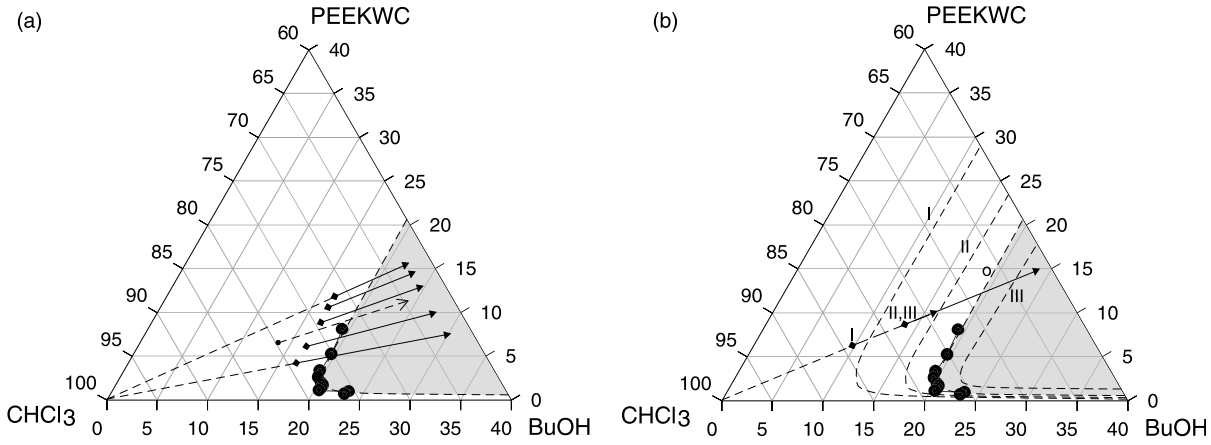

Fig. 9. (a) Phase diagram showing the influence of polymer concentration in the casting solution on the dry phase inversion process. (b) Phase diagram showing qualitatively the influence of the polymer molar mass on the phase separation. Black symbols correspond to the experimental data of the original virgin polymer (o); dashed lines correspond to the fractions I, II and III with progressively decreasing molar mass. The position of the other binodal demixing curves and the tie lines of the fractions are strictly qualitative.

described previously [16]. In this method, the appearance of turbidity by addition of nonsolvent to the clear solution and also the disappearance of turbidity by addition of solvent to the demixed system could be used for evaluation of the binodal demixing curve. Nearly perfect overlap of the data for demixing of the solution (upon nonsolvent addition) and for clearing of the demixed system (upon solvent addition) confirms that the measured data are close to the equilibrium state and that they represent the binodal demixing curve [41]. The phase diagram shows that if evaporation of the nonsolvent is negligible, then the nonsolvent/polymer ratio remains constant upon evaporation of the solvent from the cast film, as displayed schematically by the arrows in Fig. 9(a). This ratio obviously increases with decreasing polymer concentration, and is directly responsible for the higher total void fraction.

The overall thickness of the membrane is determined by two contrasting phenomena. From one side a higher polymer concentration tends to give a thicker membrane, as observed clearly from the SEM images, but from the other side the higher solids content gives a lower porosity. As expected, the mass per unit area of the membrane increases more or less proportionally with increasing polymer concentration (Table 2), if the evident experimental outlier of the 12.5% sample is not considered. This indicates that the different rheological behaviour of the solutions with increasing polymer concentration does not influence the thickness of the cast film under the given casting conditions.

3.3.2. Influence molar mass on the morphology

It was shown that the influence of the molar mass of the polymer on the rheological properties of the casting solution is similar to that of the polymer concentration. A higher molar mass increases the viscosity by incrementing the number of entanglements between the macromolecular chains in solution. This should favour the gelation of the polymer rich phase after the phase inversion has taken place, and thus stabilize the pore structure in an early stage. Indeed, Fig. 10 shows that the high molar mass sample I gives a membrane with small pores, whereas fraction III, with a much lower molar mass gives very large pores. The low molar mass also compromises the film forming properties: the membrane has a defective skin with many large pores (insert in the cross section image). The molar mass of fraction IV is so low that the polymer is extremely brittle, without any intrinsic mechanical strength, and for this reason no membranes could be formed with this polymer.

In reality, the role of the molar mass in the morphology development is much more complex than only through its influence on the viscosity and the gelation behaviour. Several contrasting effects exist. With increasing molar mass the solubility of the polymer decreases—actually the basis for the fractionation procedure—and as a result the binodal demixing curve moves to lower nonsolvent concentrations, as illustrated qualitatively in the phase diagram in Fig. 9(b). The high molar mass sample has a wider biphasic region, corresponding to a smaller polymer rich phase and a larger polymer lean phase. This should result in a higher overall porosity of the final membrane, in contrast with the experimental observations. However, the high molar mass sample also shows more rapid gelation. After gelation the possibility of pore growth is greatly reduced and further evaporation of the solvent and the nonsolvent results in a gradual shrinking of the structure. In the low molar mass sample, on the other hand, pore growth after the initial phase separation continues upon further evaporation of the solvent, resulting in larger pores. Gelation only occurs when a larger amount of solvent has evaporated.

Whether these combined effects should lead to a higher or lower overall porosity depends especially on the precise moment of gelation of the polymer rich phase and on its degree of swelling at that moment.

The molar mass further influences the membrane thickness and the mass per unit area through the rheological properties of the casting solution. At parity of polymer concentration, a higher viscosity apparently reduces the thickness of the cast

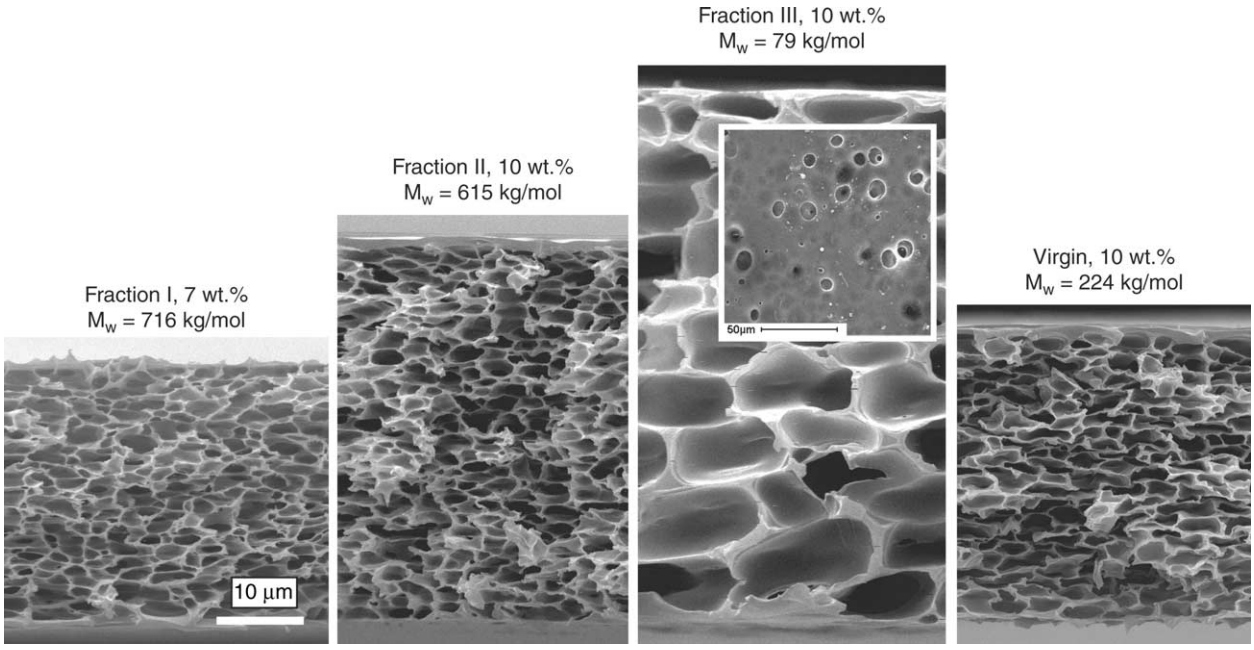

Fig. 10. SEM images of membranes obtained from polymer fractions with different molar mass and of the virgin polymer. Insert: image of the defective skin surface of fraction III.

film, as evidenced by the lower mass per unit area (samples II and III in Table 2).

3.4. Gas transport properties

In terms of performance the transport properties of the membranes are more important than their morphology. As observed by SEM, low polymer concentrations and low molar mass of the polymer give rise to a defective skin with large macropores. All other membranes present an apparently dense skin. However, permeation measurements do not always give the expected high selectivities, due to the presence of pinhole defects or microporosities. In these cases, the selectivity can nevertheless be recovered by coating of the membrane with a dilute silicone solution. The silicone blocks the pores and thus eliminates the Knudsen diffusion, without significantly influencing the transport through the dense skin [42,43]. An overview of the main results is given in Table 3.

3.4.1. Determination of the effective skin thickness

The membrane quality and effective skin thickness was evaluated by the procedure described in a previous paper [16].

Table 3
Transport properties and effective skin thickness of the membranes before and after silicone coating

		Before silicone coating						After silicone coating					
		Permeance (10^{-3} m^3/(m^2 h bar))[a]			Selectivity (–)		Effective skin[b] (µm)	Permeance (10^{-3} m^3/(m^2 h bar))[a]			Selectivity (–)		Effective skin[b] (µm)
		O_2	He	CO_2	α_{CO_2/CH_4}	α_{CO_2/N_2}		O_2	He	CO_2	α_{CO_2/CH_4}	α_{CO_2/N_2}	
concentration	5.0	–	–	–	–	–	–	–	–	–	–	–	–
virgin PEEKWC[c]	7.5	–	–	–	–	–	–	–	–	–	–	–	–
(wt%)	10.0	9.2	54.3	21.2	2.2	1.3	0.52	2.0	22.2	8.8	15.7	4.0	0.9
	12.5	1.9	25.4	9.5	19.7	4.4	0.78	1.8	23.1	9.5	31.9	5.9	0.8
	14.6	1.1	15.6	6.1	30.0	5.7	1.24	1.3	16.2	6.8	39.0	6.7	1.2
	7.5[d]	2.4	27.2	10.5	9.7	2.7	0.75	1.8	23.5	9.8	38.0	7.2	0.8
PEEKWC	I[f]	4.0	26.1	12.7	4.1	1.6	0.88	4.6	33.1	16.0	5.7	1.8	0.7
fractions[e]	II	2.7	14.4	7.0	3.1	1.4	1.76	1.1	11.5	5.5	27.1	4.0	1.6
	III	523	1125	825	0.6	0.9	–	3.7	39.8	13.7	0.6	2.3	(0.5)
	Virgin[g]	1.6	17.7	8.5	30.2	6.0	1.0	–	–	–	–	–	–

[a] 1 m^3/(m^2 h bar) = 370 GPU.
[b] From gas permeation measurements according to Eq. (6) and the method described in the text.
[c] In chloroform with 20 phr of BuOH.
[d] 16 phr of BuOH instead of 20 phr.
[e] 10 wt% of PEEKWC in chloroform and 16 phr of BuOH.
[f] 7 wt% of PEEKWC in chloroform and 11 phr of BuOH.
[g] From Ref. [1].

For each membrane x, the gas permeance $(P/L)_{x,i}$ was measured for five different gas species i (N_2, O_2, CH_4, He, CO_2). In defect free membranes or membranes with only minor defects, the gas permeance for each species through the dense skin can be described by:

$$\left(\frac{P}{L}\right)_{x,i} = \frac{P_i}{L_{x,eff}} + \frac{C_{Kn}}{\sqrt{M_i}} \quad (6)$$

in which P_i is the permeability coefficient for gas species i, $L_{x,eff}$ is the effective skin thickness, which should be independent of the gas species; C_{Kn} is a constant, depending on the surface porosity, tortuosity, pore size and temperature, and should be independent of the gas species; M_i is the molar mass of gas species i. The first term in Eq. (6) thus accounts for the solution–diffusion mechanism of the dense skin and the second term accounts for the Knudsen flux through micro-defects, if present.

Eq. (6) can then be solved for C_{Kn} and $L_{x,eff}$ if two different gases are used, allowing the correct calculation of the effective thickness of the skin, even in a defective membrane. Alternatively, one could calculate the effective thickness on the basis of only the CO_2 permeance, which is less affected by pinhole defects, introducing only a minor error. In the present work a third method was used and $L_{x,eff}$ of each membrane was calculated on the basis of the permeance data of all five gases used, by a least squares minimization procedure (standard Microsoft Excel routine), giving more reliable results than the other two methods.

3.4.2. Influence of the PEEKWC concentration

At 5 and 7.5 wt% of PEEKWC and 20 phr of butanol in the casting solution, the membrane has many macroscopic defects and is mechanically insufficiently stable to measure the gas permeance. At higher polymer concentration the membrane quality improves and the permselectivity increases with increasing polymer concentration (Table 3). The effective skin thickness is about 1 μm and seems to increase only slightly with the polymer concentration. Silicone coating gives a further improvement of the permselectivity, without affecting significantly the effective skin thickness. The highest permselectivities are obtained at 14.6 wt% of PEEKWC in the casting solution. The CO_2/CH_4 selectivity of 39 and the O_2/N_2 selectivity of 6.7 are significantly higher than the permselectivities of corresponding thick dense PEEKWC membranes, 32 and 5.9, respectively [16]. This may be due to accelerated physical ageing phenomena [44–46] or to anisotropy in the thin skin.

Simultaneous reduction of the polymer concentration from 10 to 7.5% and the nonsolvent concentration from 20 to 16 phr improves the membrane quality (Table 3). After silicone coating this membrane has a much better selectivity for oxygen than corresponding thick dense membranes have. On the basis of the thermodynamics alone (Fig. 9(a), dashed arrow), the properties of this membrane should be close to those of the membrane prepared with 10 wt% of PEEKWC and 20 phr of butanol. The better performance is due to the kinetics of the evaporation process, which increases the polymer concentration at the membrane/air interface more than in the bulk, favouring the formation of a relatively thin (0.8 μm) dense skin upon crossing of the binodal demixing curve. In order to be fully competitive with commercially available membranes that may reach permeances from about 10–100 GPU for CO_2 and 1–10 GPU for oxygen, some further reduction of the skin thickness would be desirable. Nevertheless, the O_2/N_2 selectivity (7.2) of the silicone-coated membrane is unusually high, making this membrane particularly interesting for oxygen enrichment applications. This unusually high selectivity for PEEKWC may be related to changes of the properties of thin films, for example by enhanced physical ageing [44–46]. The exact origin of this behaviour for the PEEKWC membranes will be investigated in future studies.

Also at 10 wt% of PEEKWC and 16 phr of butanol the resulting membrane is nearly defect-free and it has high a selectivity even without silicone coating (Table 3, sample 'virgin').

3.4.3. Influence of the molar mass distribution

Gas permeance measurements of the fractionated polymer samples (Table 3, bottom) confirm the morphological data. The low molar mass fractions have poor film-forming properties and/or are too brittle (fraction IV) and give macroporous membranes with low selectivity. The first fraction with the highest molar mass should have better film forming properties. However, concentrated solutions of this polymer form a gel and in addition the solution demixes at relatively low butanol concentration. Therefore a low polymer concentration and a low butanol concentration had to be used in the casting solution, resulting in a mechanically weak membrane with several defects. Since intuitively and also on the basis of the rheological data one might expect the possibility to reduce the skin thickness by using a low concentration of high molar mass polymer, further optimization of the casting procedure is desirable for this polymer fraction.

After silicone coating only the membrane from fraction II has a moderate performance; the selectivity is nevertheless somewhat lower than that of dense PEEKWC, probably due to some remaining defects. In combination with the relatively thick skin (1.6 μm) this membrane is less interesting than that prepared with the virgin polymer.

The present work shows that the virgin polymer has apparently the best combination of properties for obtaining selective GS membranes by the dry phase inversion process. It appears that a broad MMD is favourable for successful membrane formation. The high molar masses in the distribution improve the film forming properties, while the low molar masses keep the viscosity relatively low, enabling a rapid pore growth and thus the formation of a highly porous sub-layer. In addition, it allows a sufficiently high overall concentration to guarantee a defect-free dense skin.

4. Conclusions

The dry phase inversion technique was found to be a successful method for the preparation of highly selective

asymmetric gas separation membranes of PEEKWC. Under optimized conditions a thickness of the dense skin down to about 0.8 μm can be reached, giving CO_2 and oxygen permeances of 9.5×10^{-3} $m^3/(m^2\ h\ bar)$ and 1.8×10^{-3} $m^3/(m^2\ h\ bar)$, respectively (3.5 and 0.67 GPU).

In terms of permselectivity the obtained PEEKWC membranes are very interesting: the oxygen/nitrogen selectivity, α_{CO_2/N_2}, up to 7.2 and the CO_2/methane selectivity, α_{CO_2/CH_4}, up to 39, are both positioned in the upper half of the corresponding Robeson plots [15]. These values compete very well with those of typical commercial membranes, like polyimide membranes with selectivities in the range of about 5–7 for O_2/N_2 and about 30–40 for CO_2/N_2. Especially the oxygen/nitrogen selectivity of the present membranes seems particularly interesting for practical applications.

The rheological behaviour of the casting solution can be directly related to the membrane formation and morphology. A low viscosity of the casting solution, either due to the low molar mass of the polymer or to the low polymer concentration, leads to an open cellular morphology with large cells and a skin with macro-pores. A high molar mass and a high polymer concentration both increase the solution viscosity and induce the formation of a fine cellular morphology due to enhanced entanglement formation and thus accelerated gelation of the polymer rich phase upon phase inversion. Only in case of a sufficiently high solids content, i.e. at elevated polymer concentrations, the enhanced gelation effectively leads to a dense, essentially defect-free skin and a high permselectivity of the membrane. A too strong gelation of the high molar mass polymer does not allow a high solids content. Therefore a polymer with a broad MMD offers the best combination of film forming properties, pore growth and dense skin formation, and results in the best membranes with a porous sub-layer and a relatively thin dense skin.

The asymmetric membranes prepared by the dry casting process may present significantly higher selectivities than corresponding thick dense PEEKWC membranes. This might be related to enhanced physical ageing phenomena in thin films and will be subject of further studies.

Acknowledgements

We acknowledge the Italian Ministry for University, Education and Research (MIUR), for financial support.

References

[1] Mulder M. Basic principles of membrane technology. Dordrecht, The Netherlands: Kluwer; 1991.
[2] Kesting RE, Frietzsche AK. Polymeric gas separation membranes. New York: Wiley; 1993.
[3] Kesting RE. Synthetic polymeric membranes. A structural perspective. 2nd ed. New York: Wiley; 1985.
[4] Wang Z, Chen T, Xu J. J Appl Polym Sci 1997;63:1127–35.
[5] Drioli E, Zhang HC. Chimica Oggi 1989;11:59–63.
[6] Buonomenna MG, Figoli A, Jansen JC, Davoli M, Drioli E. In: Burganos VN, Noble RD, Asaeda M, Ayral A, LeRoux JD, editors. Membranes—preparation, properties and applications. MRS symposium proceedings, vol. 752; 2003, 2003. p. 3–8.
[7] Buonomenna MG, Figoli A, Jansen JC, Drioli E. J Appl Polym Sci 2004; 92:576–91.
[8] Tasselli F, Jansen JC, Drioli E. J Appl Polym Sci 2004;91:841–53.
[9] Tasselli F, Jansen JC, Sidari F, Drioli E. J Membr Sci 2005;255:13–22.
[10] Lufrano F, Drioli E, Golemme G, Di Giorgio L. J Membr Sci 1996;113: 121–9.
[11] Golemme G, Drioli E, Lufrano F. Polym Sci 1994;36:1647–52.
[12] Wang Z, Chen T, Xu J. J Appl Polym Sci 2002;83:791–801.
[13] Wang Z, Chen T, Xu J. Macromolecules 2000;33:5672–9.
[14] Wang Z, Chen T, Xu J. J Appl Polym Sci 1997;64:1725–32.
[15] Robeson LM. J Membr Sci 1991;62:165–85.
[16] Jansen JC, Macchione M, Drioli E. J Membr Sci 2005;255:167–80.
[17] Torchia AM, Clarizia G, Figoli A, Drioli E. It J Food Sci 2004;16:173–84.
[18] Jansen JC, Macchione M, Drioli E, Desalination; in press.
[19] Loske S, do Carmo Gonçalves M, Wolf BA. J Membr Sci 2003;214: 223–8.
[20] Cheng L-P, Huang Y-S, Young T-H. Eur Polym J 2003;39:601–7.
[21] Matsuyama H, Maki T, Teramoto M, Asano K. J Membr Sci 2002;204: 323–8.
[22] Yoo SH, Kim JH, Jho JY, Won J, Kang YS. J Membr Sci 2004;236:203–7.
[23] Chen RH, Hwa H-D. Carbohydr Polym 1996;29:353–8.
[24] Mikawa M, Nagaoka S, Kawakami H. J Membr Sci 2002;208:405–14.
[25] Ismail AF, Lai PY. Sep Purif Technol 2003;33:127–43.
[26] Idris A, Ismail AF, Gordeyev SA, Shilton SJ. Polym Test 2003;22: 319–25.
[27] Mendichi R, Giacometti Schieroni A. In: Pandalai SG, editor. Current trends in polymer science, vol. 6. Trivandrum, India: TWR Network; 2001. p. 17–32.
[28] Wyatt PJ. Anal Chim Acta 1993;272:1–40.
[29] Ferry JD. Viscoelastic properties of polymers. 3rd ed. New York: Wiley; 1980.
[30] Coppola L, Gianferri R, Oliviero C, Nicotera I, Ranieri GA. Phys Chem Chem Phys 2004;6:2364–72.
[31] Oliviero C, Coppola L, Gianferri R, Nicotera I, Olsson U. Colloid Surf A: Physicochem Eng Aspects 2003;228:85–90.
[32] Young RJ. Introduction to polymers. London: Chapman and Hall; 1981.
[33] Graessley WW. J Chem Phys 1967;47:1942.
[34] Bohlin L. J Colloid Interface Sci 1980;74:423–34.
[35] Winter HH, Mours M. Adv Polym Sci 1997;134:165–234.
[36] Gabriele D, de Cindio B, D'Antona P. Rheol Acta 2001;40:120–7.
[37] Coppola L, Gianferri R, Oliviero C, Nicotera I. Langmuir 2003;19: 1990–9.
[38] Coppola L, Gianferri R, Oliviero C, Ranieri GA. J Colloid Interphase Sci 2003;264:554–7.
[39] Eckelt J, Loske S, Gonçalves MC, Wolf BA. J Membr Sci 2003;212: 69–74.
[40] Schneider A, Wünsch M, Wolf BA. Macromol Chem Phys 2002;203: 705–11.
[41] It must be stressed that for highly polydisperse polymers like the present PEEKWC sample, in spite of the rather sharp turbidity change, the obtained curve is not exactly the same as the usually reported cloud point curve. The latter represents the very first appearance of turbidity and corresponds to the high molar mass species in the distribution, which are fractionated upon phase separation [40]. For the present PEEKWC solutions in chloroform, determination of the true cloud point is not unambiguous due to a slight inherent turbidity of the solution, even in the pure solvent and especially at higher polymer concentrations.
[42] Wang D, Teo WK, Li K. J Membr Sci 2002;204:247–56.
[43] Peinemann K-V, Maggioni JF, Nunes SP. Polymer 1998;39:3411–6.
[44] Shishatskii AM, Yampol'skii YuP, Peinemann KV. J Membr Sci 1996; 112:275–85.
[45] McCaig MS, Paul DR. Polymer 2000;41:629–37.
[46] McCaig MS, Paul DR, Barlow JW. Polymer 2000;41:639–48.